Can Laser Light Cool Semiconductors?

Mansoor Sheik-Bahae[1] and Richard I. Epstein[1,2]

[1]*Department of Physics and Astronomy, University of New Mexico, Albuquerque, New Mexico 87131, USA*
[2]*Los Alamos National Laboratories, Los Alamos, New Mexico 87545, USA*
(Received 14 August 2003; published 18 June 2004)

Laser cooling in semiconductors is theoretically investigated including arbitrary external efficiency and photon recycling. Experimental conditions needed to attain net cooling in GaAs are derived.

The concept of laser cooling (optical refrigeration) by luminescence up-conversion in solids dates back to 1929 [1]. Pringsheim recognized that thermal vibrational energy can be removed by anti-Stokes fluorescence if a material is excited with photons having energy below the mean fluorescence energy (see Fig. 1). Material purity problems prevented observation of this type of laser cooling until 1995, when it was first demonstrated in ytterbium-doped glass [2]. This was followed soon after by reports of cooling in dye solutions [3] and thulium-doped glass [4]. Attaining net cooling in semiconductors, however, has remained elusive. A key problem has been the inability of luminescence to efficiently escape from a semiconductor due to total internal reflection [5,6]. Although the theory of semiconductor cooling has been tackled previously [7,8], the critical issues of luminescence trapping and redshifting have not been taken into account. These processes have the potential to frustrate attempts to achieve semiconductor net cooling. Here, we resolve this problem and show that laser cooling of semiconductors is feasible.

A primary advantage of semiconductors compared to rare-earth doped solids is their potential for achieving temperatures ~10 K and below. This is due to the difference of the ground state populations in the two systems. As the temperature drops below 100 K in a rare-earth doped system, the population at the top of the ground state manifold dramatically decreases, rendering the cooling process highly inefficient. This is a consequence of Boltzmann statistics. Semiconductors, on the other hand, obey Fermi-Dirac statistics, which keeps the lower energy valence band populated even at absolute zero.

In this Letter, we describe laser cooling in semiconductor structures allowing for arbitrary external efficiency. Our analysis, for the first time, accounts for the luminescence redshift due to reabsorption. We combine this theory with the established plasma theory of semiconductor optical absorption including many-body Coulomb effects and band filling. The necessary experimental conditions for observing laser cooling in bulk semiconductor heterostructures are obtained.

We investigate an intrinsic (i.e., undoped) semiconductor system uniformly irradiated with a laser light at photon energy $h\nu$. We make the realistic assumption

that only a fraction (η_e) of the luminescence can escape the material; the remaining fraction ($1 - \eta_e$) is trapped and reabsorbed, which causes the reexcitation of electron-hole pairs and subsequent reemission. This is known as photon recycling. For steady-state conditions at a given temperature, the electron-hole (*e-h*) carrier density (*N*) is obtained from the following equation:

$$0 = \frac{\alpha(\nu, N)}{h\nu}I - AN - BN^2 - CN^3 + (1 - \eta_e)BN^2, \tag{1}$$

where I is the laser irradiance and $\alpha(\nu, N)$ is the interband absorption coefficient. Density dependent absorption results from (i) Coulomb screening and (ii) band filling. The latter effect is saturation due to the Pauli exclusion principle (i.e., Pauli band blocking). It is accounted for by taking $\alpha(N, h\nu) = \alpha_0(N, h\nu)\{f_v - f_c\}$, where α_0 is the unsaturated absorption coefficient [9]. The bracketed term is the band-filling factor defined by the Fermi distribution functions f_v and f_c for the valence and conduction bands, respectively. The recombination processes are nonradiative (AN), radiative (BN^2), and Auger (CN^3). All the above coefficients are temperature dependent. Rearranging the terms in Eq. (1) yields a radiative recombination rate that scales as $\eta_e B$. A similar result has
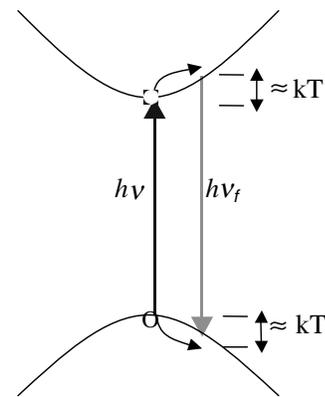
FIG. 1. Cooling cycle in laser refrigeration of a semiconductor in which a laser photon with energy $h\nu$ is absorbed followed by emission of an up-converted luminescence photon at $h\nu_f$.

been derived by Asbeck [10]. It is important to emphasize that η_e is averaged over the entire luminescence spectrum, i.e., $\eta_e = \int S(\nu)R(\nu)\,d\nu / \int R(\nu)\,d\nu$. Here $S(\nu)$ is the geometry-dependent escape probability and $R(\nu)$ is the luminescence spectral density, which is related to the absorption coefficient through the van Roosbroeck-Shockley relation [11]. The radiative recombination is obtained from $BN^2 = \int R(\nu)\,d\nu$ [9].

The net optical power deposited in the semiconductor is the difference between the absorbed power and escaped luminescence:

$$P_{\text{net}} = \eta_e BN^2(h\nu - h\tilde{\nu}_f) + ANh\nu + CN^3 h\nu + \Delta P, \tag{2}$$

where we define an "escaped" mean luminescence photon energy $h\tilde{\nu}_f = \int S(\nu)R(\nu)h\nu\,d\nu / \int S(\nu)R(\nu)\,d\nu$. A residual heating term ΔP accounts for free-carrier absorption and other parasitic absorptive processes. Equation (2) completely describes laser cooling of a semiconductor. It incorporates luminescence trapping via inhibited radiative recombination ($\eta_e B$) and includes redshifting of the escaped luminescence $h\tilde{\nu}_f$.

In the limit of high external efficiency where $S(\nu) = 1$, Eq. (2) approaches previous results that assume $\eta_e = 1$ and $\tilde{\nu}_f = \nu_f$ [5,7,8]. Equation (2) indicates laser cooling occurs when $P_{\text{net}} < 0$, which requires a dominant contribution from radiative recombination. Cooling efficiency η_c is defined as the ratio of cooling power density $P_c = -P_{\text{net}}$ to the absorbed laser power density ($P_{abs} = \alpha I + \Delta P$). Ignoring the ΔP contributions for the moment, η_c is

$$\eta_c = \bar{\eta}_i \frac{\tilde{\nu}_f}{\nu} - 1, \tag{3}$$

where $\bar{\eta}_i = \eta_e BN^2/(AN + \eta_e BN^2 + CN^3)$ describes the "inhibited" or external radiative quantum efficiency. Assuming the radiative term dominates recombination (i.e., $\eta_e B/C > N > A/\eta_e B$) and ignoring band filling, we can analytically solve for optimum carrier density and incident laser irradiance. We account for parasitic absorption by taking $\Delta P = \alpha_b I + \sigma_{fca} NI$, where α_b represents background parasitic absorption from defects and impurities and σ_{fca} is the free-carrier absorption cross section. Net cooling ($P_{\text{net}} < 0$) occurs if $A < A_0$, where A_0 defines a "break-even" nonradiative recombination rate:

$$A_0 = \left(\eta_q - \frac{\alpha_b}{\alpha(\nu)}\right)^2 \frac{(\eta_e B)^2}{4C'}. \tag{4}$$

where we have defined a quantum cooling efficiency $\eta_q = (h\tilde{\nu}_f - h\nu)/h\nu$ and $C' = C + \sigma_{fca}\eta_e B/\alpha(\nu)$. Cooling takes place for a laser irradiance in the range $I_1 < I < I_2$, where $I_{1,2} = \{h\nu\eta_e B/\alpha(\nu)\}N_{1,2}^2$, and the e-h densities are

$$N_{1,2} = \sqrt{\frac{A_0}{C'}}\left(1 \mp \sqrt{1 - \frac{A}{A_0}}\right). \tag{5}$$

Inclusion of band filling, however, will limit the maximum carrier density attainable with optical pumping ($N_{\max}$) that occurs when $f_c = f_\nu$. As we discuss below, cooling may be inhibited at low temperature, where N_1 can approach and even exceed $N_{\max}$. The parameters B and C are fundamental properties of a semiconductor; these coefficients can be calculated and measured for bulk or quantum-confined structures. Reported values, however, vary considerably. In bulk GaAs, for example, the numbers range from $2 \times 10^{-16} < B < 7 \times 10^{-16}\,\text{m}^3/\text{s}$ and $1 \times 10^{-42} < C < 7 \times 10^{-42}\,\text{m}^6/\text{s}$. To assess the feasibility of laser cooling, we use average values in our calculations: $B = 4 \times 10^{-16}\,\text{m}^3/\text{s}$ and $C = 4 \times 10^{-42}\,\text{m}^6/\text{s}$ and initially ignore background and free-carrier absorption. The break-even nonradiative lifetime at room temperature $\tau_{nr}^0 = 1/A_0$ is plotted in Fig. 2 as a function of η_e. We set $h\nu_f - h\nu = kT$ and use the mean luminescence wavelength of $\lambda_f \sim 860$ nm. The gray area under the curve designates the undesired heating region. The horizontal line corresponds to $\tau_{nr} = 40\,\mu$s, which is the longest reported nonradiative lifetime in a GaAs/InGaP double heterostructure, although 5–10 μs is typical [12]. These lifetimes set a lower limit on extraction efficiency $\eta_e = 15\%$ for the best material; in practice 20%–30% may be required.

Equation (4) suggests increasing the quantum efficiency η_q by decreasing the incident photon energy reduces the break-even lifetime. At $h\nu_f - h\nu = 2\,kT$, for example, the required lifetime decreases by a factor of 4. As the photon energy moves into the Urbach tail, however, the interband absorption drops rapidly and therefore background and free-carrier absorption are no longer negligible. Recently, it was found that σ_{fca} at band-edge wavelengths is much smaller than previously expected [13]. For GaAs, $\sigma_{fca} \approx 10^{-24}\,\text{m}^2$, which requires $\alpha(\nu) \gtrsim 10^3\,\text{m}^{-1}$ to ensure that free-carrier losses are
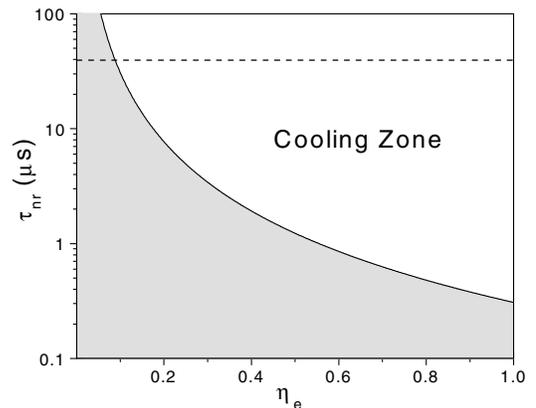
FIG. 2. The break-even nonradiative lifetime as a function of the luminescence extraction efficiency in bulk GaAs at 300 K. This calculated lifetime delineates the cooling zone and heating zone (shaded area). The horizontal dashed line corresponds to $\tau_{nr} = 40\,\mu$s, the longest lifetime reported in a GaAs/InGaP double heterostructure.

negligible compared to Auger recombination (i.e., $C' \approx C$). This condition is satisfied even at $\lambda = 890$ nm (corresponding to $h\nu_f - h\nu = 2$ kT), where $\alpha(\nu) \approx 10^4$ m^{-1}. Therefore, free-carrier absorption does not present a major limitation to laser cooling. Possible sources for α_b are (i) impurity absorption in active and/or cladding layers and (ii) substrate absorption. It is also important that α_b in Eq. (4) be scaled to the device geometry: $\alpha'_b = \alpha_b \times (d/L)$, where d and L are the thicknesses of the lossy and active media, respectively. For an active medium $L \approx 1$ μm and substrate thickness of 1 cm, this requires $\alpha(\nu) > 10^5 \alpha'_b$. This, in turn, demands $\alpha'_b < 10$ m^{-1} at $\lambda = 870$ nm, and $\alpha'_b < 0.1$ m^{-1} at $\lambda = 890$ nm. A ZnS substrate with $\alpha'_b \lesssim 10^{-2}$ m^{-1} meets such a requirement. A ZnSe substrate having $\alpha'_b \lesssim 0.3$ m^{-1} can be effective only at $\lambda \approx 870$ nm [14]. We shall later discuss using such substrates to make index-matching dome lenses to enhance η_e.

Our analysis to this point has been concerned only with net cooling from room temperature. Of key importance is determining a break-even lifetime for cryogenic conditions. Using the expected scaling $C(T) \propto \exp(1 - 300/T)$ [15], $B \propto T^{-3/2}$ [9,16], keeping $\eta_q \approx kT/E_g$, and ignoring parasitic losses and the small temperature dependence of the band-gap energy, we obtain

$$\frac{A_0(T)}{A_0(300)} \simeq \left(\frac{300}{T}\right)\exp\left(\frac{300 - T}{T}\right). \quad (6)$$

This indicates that at $T = 100$ K, for example, the break-even nonradiative lifetime is lowered by ~ 20 times compared to room temperature. Furthermore, nonradiative recombination is primarily surface recombination, which decreases exponentially with temperature [16]. This makes observation of laser cooling even more favorable at a lower starting temperature, despite decreased efficiency ($\approx kT/E_g$). Reduced cooling efficiency at a lower temperature is primarily due to the smaller probability for phonon absorption by electrons and holes. This is manifest in a temperature-dependent exciton linewidth [9]:

$$\Gamma(T) = \Gamma_0 + \sigma T + \gamma N_{\mathrm{LO}}(T), \quad (7)$$

where Γ_0 is due to an inhomogeneous background distribution of impurities, σ is the contribution from acoustic phonon scattering, γ is the coefficient of LO-phonon scattering, and $N_{\mathrm{LO}}(T)$ is the Bose-Einstein phonon distribution. Exciton-exciton scattering is negligible at the densities encountered here [17]. At lattice temperatures approaching 10 K, the acoustic phonon component dominates and the scattering rate becomes comparable to the radiative recombination rate (BN^2). This means that cold exciton recombination occurs before complete thermalization with the lattice. Hot exciton recombination is a similar process that has hindered observation of Bose-Einstein condensation in semiconductors. This problem has been significantly alleviated by employing quantum-confined systems where relaxation of wave-vector con-

servation in the confined direction reduces σ by nearly 3 orders of magnitude [18]. Quantum confinement may allow realization of semiconductor cooling below 10 K.

Band filling can saturate long wavelength absorption because of the lower density of states near the band edge. To estimate its importance in semiconductor cooling, we calculate N_1 using the same parameters as in Fig. 2; we assume an external efficiency $\eta_e = 20\%$ and temperature-independent nonradiative lifetime $1/A = 10$ μs. The maximum attainable density is $N_{\max} \sim 25N_1$ at 300 K, dropping to $N_{\max} \sim 2.5N_1$ at 30 K, with insufficient excitation for cooling predicted at 10 K. This worst case estimate ignores reduced nonradiative recombination and overestimates excitonic saturation at low temperature. A more accurate model of band filling requires a rigorous description of exciton absorption and luminescence in the presence of many-body interactions.

We now analyze the effect of radiation trapping and photon recycling in laser cooling of GaAs. Luminescence removal is facilitated by a nearly index-matched dome attached to the heterostructure [Fig. 3(a)] [5]. Domes made from ZnS or ZnSe are transparent in the infrared and present a minimal heat load from blackbody radiation; they do not significantly limit the amount of cooling that can be attained. Two heterostructure designs have been suggested for improving the efficiency of light emitting diodes as depicted in Fig. 3(b). In Structure I, both surfaces are polished, which limits the radiation escape cone to the angle of total internal reflection. For Structure II, the bottom surface is textured to statistically randomize the photon trajectories. More light rays avoid the total internal reflection condition and escape via photon recycling. Ignoring Fabry-Perot effects, escape probabilities for both cases have been evaluated with statistical geometric optics using solid-angle averaging in a photon-gas model [19]. Sample thickness (L), absorption, and refractive index enter the calculation through
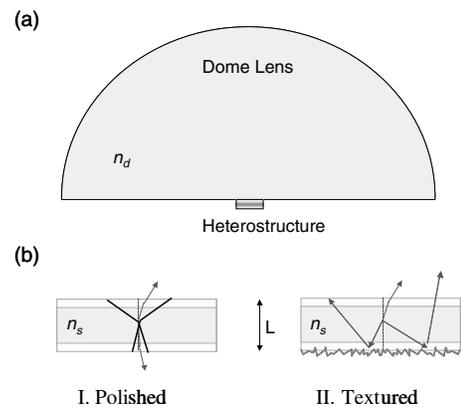
FIG. 3. (a) A high index (n_d) dome is bonded to a semiconductor heterostructure of index n_s consisting of a GaAs active layer sandwiched between two thin layers of AlGaAs or InGaP for surface passivation. (b) Heterostructure designs with polished planar surfaces (I) and a textured bottom surface (II).
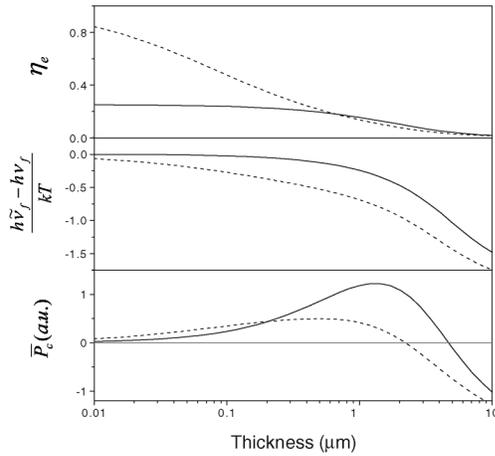
FIG. 4. Calculated escape efficiency (top), redshifting of the escaped mean luminescence photon energy (middle), and total cooling power (bottom) as a function of the GaAs thickness for Structure I (solid lines) and Structure II (dashed lines) depicted in Fig. 3. A density of 5×10^{17} cm^{-3} and $T = 300$ K are assumed.

the previously defined escape parameter $S(\nu)$. Taking the thickness of the active GaAs as the independent parameter, we analyze these systems assuming a ZnS dome with index of refraction $n_d = 2.4$. ZnS has extremely low optical absorption in the spectral region of interest.

To evaluate the luminescence spectrum, $R(\nu)$, we use an analytical plasma theory that has shown good agreement with experimental results for $T > 70$ K [20]. The calculated escape efficiency (η_e) and shift of escaped mean luminescence energy are shown in Fig. 4. Results are presented for $L > 0.01$ μm where quantum confinement of carriers is not important. Photon recycling provided by the textured-surface structure results in much higher escape efficiency as the thickness is reduced. This enhanced efficiency is obtained at the expense of deleterious redshifting of the luminescence spectrum—lower energy photons suffer less absorption and can eventually escape. A polished (planar) surface exhibits a relatively flat efficiency up to thickness 1 μm and the mean escaped photon energy remains close to the internal value of $h\nu_f$. Samples with thickness $L > 0.6$ μm are larger than the photon mean-free path; both surfaces then provide essentially the same efficiency. A quantity of interest for applications is the cooling power. We define a normalized cooling power by assuming a fixed excitation energy at $h\nu = h\nu_f - kT$ in Eq. (2):

$$\bar{P}_c = K\eta_e(h\tilde{\nu}_f - h\nu)V \approx K\eta_e(kT - \Delta\epsilon)V, \quad (8)$$

where K is a normalization constant, $\Delta\epsilon = h\nu_f - h\tilde{\nu}_f$ is the amount of luminescence photon energy shift, and $V =$ Area $\times L$ is the illumination/recombination volume. We evaluate this quantity ($\bar{P}_c$) for both geometries as a

function of the thickness as shown in Fig. 4. Highest cooling power and, hence, lowest temperature is achieved with a polished structure of thickness of 1–2 μm. If highest cooling efficiency is desired and/or a large η_e is required to achieve the break-even condition, a thin ($L < 500$ nm) textured-surface structure is advantageous.

In summary, we have developed a model to treat laser cooling in semiconductors for arbitrary external efficiency. The break-even nonradiative lifetime and luminescence extraction efficiency are obtained. Photon recycling causes luminescence reabsorption and redshift, which may adversely affect cooling in textured-surface structures. Highest cooling power is achieved with polished planar structures and index-matching encapsulation.

[1] P. Pringsheim, Z. Phys. 57, 739 (1929).
[2] R. I. Epstein et al., Nature (London) 377, 500 (1995).
[3] J. L. Clark and G. Rumbles, Phys. Rev. Lett. 76, 2037 (1996).
[4] C.W. Hoyt et al., Phys. Rev. Lett. 85, 3600 (2000).
[5] H. Gauck et al., Appl. Phys. A 64, 143 (1997).
[6] E. Finkeissen et al., Appl. Phys. Lett. 75, 1258 (1999).
[7] A. N. Oraevsky, J. Russ. Laser Res. 17, 471 (1996).
[8] L. A. Rivlin and A. A. Zadernovsky, Opt. Commun. 139, 219 (1997).
[9] P. K. Basu, Theory of Optical Processes in Semiconductors (Oxford, New York, 1997).
[10] P. Asbeck, J. Appl. Phys. 48, 820 (1977).
[11] W. van Roosbroeck and W. Shockley, Phys. Rev. 94, 1558 (1954).
[12] J. M. Olson et al., Appl. Phys. Lett. 55, 1208 (1989).
[13] A. Haug, Semicond. Sci. Technol. 7, 373 (1992).
[14] B. Imangholi et al., Opt. Commun. 227, 337 (2003).
[15] G. P. Agrawal and N. K. Dutta, Long-wavelength Semiconductor Lasers (Van Nostrand-Reinhold, New York, 1986).
[16] G. t'Hooft and C. Vanopdorp, Appl. Phys. Lett. 42, 813 (1983).
[17] A. C. Schaefer and D. G. Steel, Phys. Rev. Lett. 79, 4870 (1997).
[18] L. V. Butov et al., Nature (London) 417, 47 (2002).
[19] I. Schnitzer et al., Appl. Phys. Lett. 62, 131 (1993).
[20] H. Haug and S.W. Koch, Quantum Theory of the Optical and Electronic Properties of Semiconductors (World Scientific, Singapore, 1994).